Recent advances in molecular imaging biomarkers in cancer: application of bench to bedside technologies

Roy van der Meel[1], William M. Gallagher[2,3], Sabrina Oliveira[4], Aisling E. O'Connor[2], Raymond M. Schiffelers[1] and Annette T. Byrne[3,5]

[1] Department of Pharmaceutics, Utrecht Institute for Pharmaceutical Sciences, Faculty of Science, Utrecht University, Sorbonnelaan 16, 3584 CA, Utrecht, The Netherlands
[2] UCD School of Biomolecular and Biomedical Science, UCD Conway Institute, University College Dublin, Belfield, Dublin 4, Ireland
[3] OncoMark Limited, NovaUCD, Belfield Innovation Park, University College Dublin, Belfield, Dublin 4, Ireland
[4] Cellular Dynamics, Department of Biology, Faculty of Science, Utrecht University, Padualaan 8, 3584 CH, Utrecht, The Netherlands
[5] Department of Physiology & Medical Physics, Royal College of Surgeons in Ireland, Reservoir House, Sandyford Industrial Estate, Ballymoss Road, Dublin 18, Ireland

Molecular imaging is the visualization, characterization and measurement of biological processes at the molecular and cellular level. In oncology, molecular imaging approaches can be directly applied as translational biomarkers of disease progression. In this article, selected imaging modalities are discussed with respect to this role. Recent studies focusing on emerging imaging biomarkers and new developments in the field are highlighted. Importantly, because *ex vivo* or tissue-based imaging now represents an important tool in the discovery and validation of oncology biomarkers, special attention is given to this resurgent field.

Introduction

In recent years, an important tenet of oncology research has been to develop new tumor-targeted therapies and diagnostic approaches for the early detection of malignancies. A crucial component in these activities has been the discovery and validation of new oncology biomarkers. The Biomarkers Definitions Workgroup, sponsored by the National Institutes of Health, stated in 2001 that 'a biological marker – biomarker – is a characteristic that is objectively measured and evaluated as an indicator of normal biological processes, pathogenic processes, or pharmacologic responses to a therapeutic intervention' [1]. Currently, clinical size measurements of tumor lesions by computed tomography (CT) and magnetic resonance imaging (MRI) are the predominant ways in which disease progression and therapeutic drug efficacy are assessed. Indeed, criteria determined by the World Health Organization (WHO) [2] and according to the Response Evaluation Criteria in Solid Tumors (RECIST) [3,4] classification system are based on uni-dimensional and bi-dimensional measurements of tumor size. At present, overall response and progression-free survival are the only imaging biomarkers used as surrogate endpoints to assess the effects of chemotherapy and radiation therapy in clinical trials.

It is now known that although certain novel therapies might induce small alterations in tumor size [5], these changes might not be easily detected and classified by the WHO and RECIST classification system. For example, measuring treatment response by using RECIST in patients with metastatic gastrointestinal stromal tumors treated with imatinib led to underestimation of therapeutic effect [6]. Therefore, new imaging biomarkers that follow disease progression and detect therapeutic response at a molecular and cellular level are required. Furthermore, imaging biomarkers can be used to select appropriate patient types for novel targeted therapies.

Molecular imaging (MI) enables non-invasive monitoring of cellular processes at a molecular or genetic level *in vivo*. In this way, MI modalities can be used directly in oncology as biomarkers of disease progression. Furthermore, the effect of new targeted anti-cancer therapies on cellular pathways and gene expression can also be monitored. Technological advances in the imaging hardware, as well as developments in the variety of contrast agents

Corresponding author:. Byrne, A.T. (annette.byrne@rcsi.ie)

1359-6446/06/$ - see front matter doi:10.1016/j.drudis.2009.12.003

or tracers available, have resulted in an increasing role for MI in tumor diagnosis, monitoring tumor progression and the assessment of therapeutic effect. Tissue-based or *ex vivo* imaging has also now emerged as an important tool in the discovery and validation of oncology biomarkers in preclinical research. Distribution of biomolecules such as proteins can be visualized by infrared spectroscopy and spectrometry-based imaging without prior labeling. Furthermore, technological developments have lead to automated image analysis of tissue specimens, enabling recognition and quantitation of oncology biomarkers.

This short review discusses the integrated role of selected imaging modalities as disease progression biomarkers in oncology. Particular attention will be paid to the latest and most exciting developments in the oncology biomarker imaging field with a special focus on the application of state-of-the art tissue-based imaging approaches towards biomarker discovery and validation.

Molecular imaging biomarkers to monitor disease progression

Optical imaging: bioluminescence and fluorescence

Bioluminescence imaging (BLI) relies on the production of light following an enzymatic reaction of luciferase with its substrate (luciferin or coelenterazine), which can be visualized with an external detector. Luciferase oxidizes luciferin in the presence of ATP and molecular oxygen to form an electronically excited oxy-luciferin species. Visible yellow-green to yellow-orange light is emitted after relaxation of excited oxy-luciferin to its ground state. In general, cells can be transfected *in vitro* to express luciferase before inoculating animals. In addition, reporter gene expression can be introduced through the germline to generate bioluminescent transgenic tumor models. Luciferase expression can be visualized after injection of substrate. Clearly, because genetically expressed luciferase is a fundamental requirement of BLI, its application is currently limited to the preclinical setting [7]. In this instance, however, it has several advantages over other molecular imaging techniques. First, BLI is relatively cost effective and user friendly and allows for high-throughput screening. Furthermore, BLI is a non-invasive imaging technique and enables longitudinal monitoring of disease progression within the same animal. In this way, each animal can function as its own control, decreasing the amount of animals needed for a study and reducing costs. Finally, BLI is a non-radioactive image modality, in contrast to positron emission tomography (PET) or single photon emission computed tomography (SPECT). In comparison to nuclear imaging, BLI is not an absolutely quantitative imaging approach. However, it does enable monitoring and accurate measurements of tumor growth dynamics by quantification of relative light emission changes over time. Therefore, BLI produces images which supply measurements of tumor growth that are neither subjective or qualitative.

BLI has been applied extensively to preclinical cancer models. Most simple BLI-based oncology research has used luciferase-expressing xenograft models to study tumor progression [83]. For example, studies have been performed to examine the possibility of using dynamic BLI to determine the effects of the vascular disrupting agent combretastatin A4 phosphate on human breast tumor xenografts in mice. BLI was useful in monitoring the effects of combretastatin A4 phosphate on the tumor vasculature, which was confirmed by dynamic contrast-enhanced MRI (DCE-MRI) and histology [8]. Nevertheless, genetically engineered luciferase reporter mouse models (GEMMs) have also been developed that facilitate the study of spontaneous tumorigenesis under a variety of conditions. Although these models lack environmental influences associated with human cancer development, GEMMs represent the most accurate models of tumorigenesis currently available. For example, a bigenic transgenic reporter mouse model was designed to monitor local and metastatic prostate tumor growth. Transgenic mice with luciferase gene expression restricted to the prostate were crossbred with transgenic adenocarcinoma mouse prostate mice, creating a model dependent on functional androgen receptor expression [9]. Some GEMMs rely on site-specific recombinases to irreversibly switch on or off gene expression in a cell type-specific manner. Tumor suppressors can be switched off and oncogenes switched on, resulting in tumorigenesis. The development of conditional reporters has made it possible to visualize spontaneously arising tumors in such models using BLI. One example of this is the use of the Cre/loxP system to conditionally 'switch on' bioluminescence. Theoretically, this reporter facilitates the imaging of any Cre-dependent tumor irrespective of tissue and has shown demonstrable utility in the imaging of a conditional PTEN (tumor suppressor gene)-dependent prostate adenocarcinoma model [10]. This prostate model is also unique because luciferase expression is prostate specific but completely independent of androgens.

TABLE 1

Summary of key fluorescence imaging biomarker studies

Fluorescent probe	Approach	Purpose	Refs
ICG	NIRF imaging of a nanocarrier system in xenograft mouse models of pancreatic, hepatocellular and lung carcinoma	Feasibility of nanocarrier as a tumor imaging agent	[13]
Alexa 750	NIRF imaging of nanocarrier system in a syngeneic mouse model of breast cancer	Monitor tumor progression	[14]
Alexa 750	NIRF imaging of affibodies in a xenograft mouse model of breast cancer	Detect HER2-positive tumors	[66]
QD	NIRF imaging of a QD coupled to EGF in a xenograft mouse model for colon cancer	Development and validation of an imaging probe to discriminate between tumor and healthy tissue	[12]
MB	Imaging of a photodynamic MB in a xenograft mouse model for epithelial carcinoma	Tumor detection and assessment of therapeutic efficacy of photosensitizing agent	[15]
ProSense 680	Combination of fluorescent molecular tomographic imaging and MRI in a xenograft mouse model for glioma	Tumor detection and assessment of therapeutic effect of chemotherapy	[18]

Light production in fluorescence imaging is based on the excitation of a fluorescent molecule with visible light, resulting in emitted light of lower energy and longer wavelength that can be used for imaging purposes. Although extensively used *in vitro*, use of fluorescence imaging *in vivo* is limited by the depth of tissue penetration of light [11]. Nevertheless, notable advances have been made in translating this technology over the past several years making use of long-wavelength tissue-penetrating light.

Recently developed applications have used fluorescence to monitor tumor progression using near-infrared fluorescence (NIRF) probes, quantum dots (QDs) and molecular beacons (MBs) (Table 1). Such fluorophores can be further coupled to a biologically active molecule, such as proteins [12] or even active therapeutics.

NIRF makes use of the near-infrared spectrum, enabling deeper tissue penetration of light. An increasing number of studies demonstrate the utility of NIRF *in vivo*: most recently, the NIRF dye indocyanine green, or ICG (light emission 790 nm), has been coupled to a nanocarrier for tumor imaging. Human hepatocellular carcinoma cells expressing luciferase were injected in mice, establishing a model for liver tumors. ICG-coupled nanocarrier was subsequently delivered parenterally. The ICG NIRF fluorescence distribution pattern overlapped with the luciferin bioluminescence, demonstrating the potential of the NIRF-coupled nanocarrier as an imaging agent and possible drug delivery system for hepatic tumors [13]. In another approach, the Alexa 750 NIRF dye has been coupled to phospholipid micelles to detect tumors in a syngeneic mouse model for breast cancer. The passively targeting micelles enabled rapid imaging of the tumor because the tumor-specific signal was considerably higher than the surrounding tissue, thus demonstrating potential as a contrast agent imaging biomarker for tumor detection [14].

Fluorescent QDs are nanocrystals made from inorganic semiconductor materials. Although they are considerably larger than common fluorescent dyes, inherent features such as brightness, photostability and a wide absorption/small emission band have encouraged a growing interest in the application of QDs for *in vivo* imaging purposes. One approach has been to use phospholipid micelles loaded with QDs (NIRF-emitting cadmium selenide; light emission 790 nm) for tumor detection. Whole-body imaging of mice bearing syngeneic breast tumors showed clear and rapid tumor imaging and biodistribution of QD micelles. One area of concern, however, is that utilization of QDs is limited by toxicity issues, such as degradation of toxic metals in cells [12].

MB imaging represents a novel method of monitoring gene nucleic acid or protein expression. MBs are hairpin-shaped molecules with an internally quenched fluorophore, of which the loop region is designed to be a complementary sequence to the target molecule. Upon binding of the target molecule, fluorophore fluorescence is restored. A recent study has demonstrated the potential of MBs for cancer detection and treatment. A photodynamic MB containing a fluorescent photosensitizer was designed; this MB targets fibroblast activation protein (FAB), which is highly expressed on cancer-associated fibroblasts of human epithelial carcinoma but not on normal fibroblasts. Mice bearing HEK xenografts expressing FAB showed a significantly higher fluorescence signal than HEK xenografts that did not express FAB. Furthermore, the therapeutic potential of the MB was shown *in vitro*. The MB was non-toxic in the absence of light but showed significant photo-

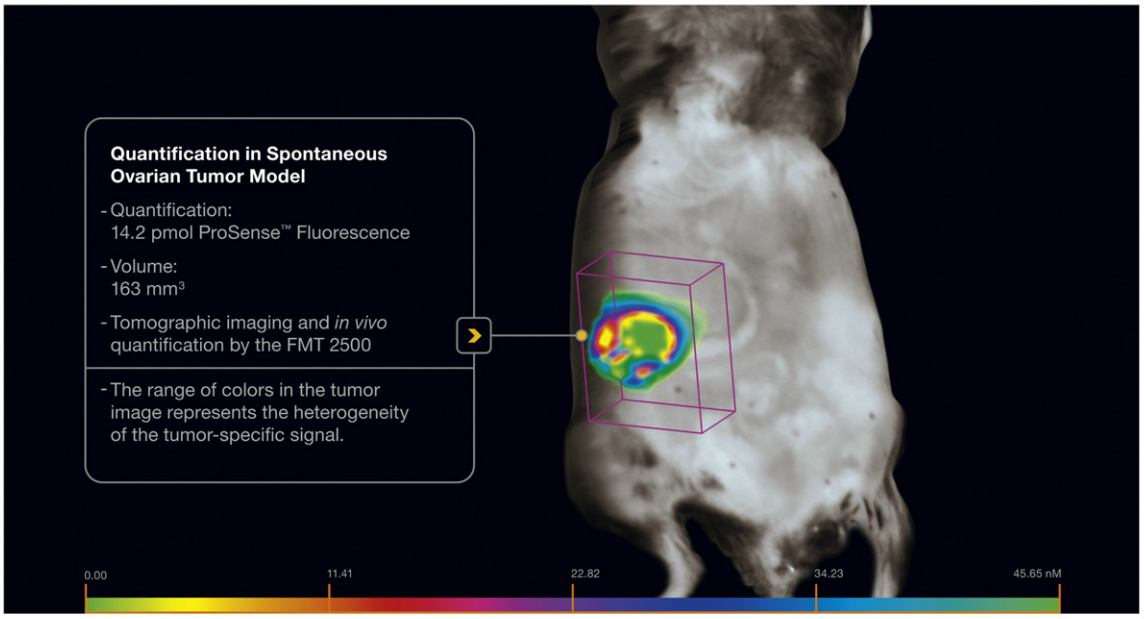

FIGURE 1

Quantification of spontaneous ovarian tumor model using FMT quantitative tomography and ProSense imaging probe. Color range in tumor represents the heterogeneity of tumor-specific signal. Prosense (14.2 pmol) was parenterally delivered and animals imaged using the FMT 2500 quantitative tomography system (Visen). Image courtesy of D. Connolly, M. Clapper and H. Hensley, Fox Chase Cancer Centre.

toxicity in HEK cells expressing FAB (whereas no toxicity was seen in HEK cells that did not express FAB) [15].

Several advanced 'activatable' optical imaging biomarkers are currently under development by the US imaging company VisEn, a key commercial developer of fluorescence *in vivo* imaging technologies. One such imaging biomarker platform, the NIRF ProSense fluorescence imaging, is activated *in vivo* by lysosomal cathepsin proteases that have been shown to be important in multiple disease processes [16,17].

ProSense 680 and 750 have absorption maxima at 680 nm and 750 nm, respectively. To date, much progress has been made with respect to tumor imaging using ProSense in the context of 3D fluorescence molecular tomography (FMT). One of the key limitations of optical imaging is the natural scattering of photons by biological tissue. As a result of this scattering, the 2D fluorescent signal at the surface of an imaging subject does not correlate with the true fluorescent signal intensity emanating from within the subject. To solve this problem, FMT technology uses specific lasers to trans-illuminate a subject from multiple different positions on one side. A camera positioned on the opposite side collects both laser excitation and agent fluorescence information. Normalization of agent fluorescence by laser excitation signal provides an essential compensation for differences in optical properties owing to tissue heterogeneity throughout the subject's body (e.g. absorption differences between heart, liver, lungs, and so on). By illuminating the subject from multiple positions, FMT imaging systems use an algorithm that models light propagation through tissue and acquires sufficient depth information to calculate the location and concentration of fluorescence within the three-dimensional space of the subject. Thus, orthotopic tumors in deep anatomical sites such as the thymus, ovaries, brain and colon are readily accessible by FMT. In short, this technology facilitates the detection and quantification of deep tissue tumor growth, disease progression and metastases, and therapeutic treatment efficacy. Imaging of the ProSense molecule using FMT provides pmol readouts of localized ProSense, as well as the volume of fluorescent signal in mm^3 [18] (Figure 1).

Extensive data have also been recently generated that characterize breast cancer metastasis to the lung, progression of lung tumor growth and a dose-responsive decrease in signal associated with cytotoxic therapies, in agreement with standard metrics of tumor burden [18,19]. In a recent collaboration with researchers at the Fox Chase Cancer Centre, spontaneous development of ovarian cancer (TgMISIIR-TAg mice) was imaged with a variety of VisEn optical imaging biomarkers designed to assess vascular leak, matrix metalloproteases activity and cathepsin activity (D. Connolly, M. Clapper, H. Hensley, unpublished data). ProSense detected viable tumor tissue in affected ovaries and provided images of deep tissue localization and robust fluorescence quantification.

PET imaging

PET imaging is fundamentally based on the detection of pairs of gamma rays. These gamma rays are produced when a positron emitted by a PET tracer encounters an electron. This encounter results in a pair of 511 keV gamma rays that, emitted in opposite directions, can be detected by a scintillator. This, in turn, generates light, which is picked up by a photodetector. CT is used to generate a 3D image of tracer concentration at a given location. Like PET, SPECT imaging is also based on imaging of gamma rays. However, SPECT tracers directly emit gamma radiation. A gamma camera is rotated around a subject to obtain multiple 2D images of SPECT tracer distribution. A 3D image is generated by computer-processed tomographic reconstruction of the 2D image dataset.

A tracer can be defined as a positron-emitting (PET) or gamma-ray-emitting (SPECT) radionuclide coupled to a biologically functional molecule (biomarker). The most extensively used PET tracer is the glucose analogue ^{18}fluorine-2-deoxy-D-glucose (FDG). Because many tumors have an increased glucose uptake, FDG is taken up by malignant cells and phosphorylated by hexokinase. As a result, FDG is trapped in the cell and can be detected by PET imaging. PET produces higher-resolution images than SPECT; however, SPECT scans are less expensive. Combinations of PET and SPECT with CT can increase the anatomical resolution of scans. PET-CT with FDG is now commonly used in the clinic and will certainly be used when more recent tracers, such as ^{18}F-3-fluoro-3-deoxy-thymidine (FLT), translate to the clinic. The usefulness of applying such a multimodality approach in monitoring cancer progression or therapeutic efficacy is now well established [20,21]. Drawbacks of PET/SPECT include the use of radioactive isotopes and the requirement for an on-site cyclotron. Furthermore, the choice of tracer can influence imaging results because of their differing half lives and varying intracellular fates. For example, FDG has low sensitivity for slow-growing tumors and high uptake levels in the brain [22]. Finally, because all PET tracers are injected intravenously, it is essential that the interaction between the tracer and its target is properly validated to avoid measuring surrogates of blood flow.

As discussed previously, FGD PET has several limitations; thus, several highly specific PET tracers are now emerging in an effort to improve the application of PET imaging as biomarker in oncology. PET tracers can be broadly divided into three groups, based on their biological tumor target: tumor metabolism, tumor hypoxia and tumor receptor over-expression. Table 2 summarizes key PET biomarker imaging studies over the past several years.

Tumor metabolism

In cases in which FDG PET imaging might be impaired, PET tracers based on different biological processes are required. Next to increased glucose metabolism, which is the basis of FDG PET imaging, tumor cells also show increased amino acid metabolism. Therefore, radiolabeled amino acids have been developed as PET tracers. An example is L-[methyl-^{11}C] methionine (MET).

Kracht *et al.* [23] have demonstrated MET PET imaging in patients with suspected primary or recurrent brain tumors. MET PET was performed before stereotactic biopsy. A new method was developed that facilitated biopsy trajectory plotting in PET images, and in this way, an accurate comparison of PET and histopathological data could be performed. It was concluded that MET PET can detect solid brain tumor tissue as well as infiltrating tumor parts with high sensitivity and specificity [23].

In patients with astrocytomas, tumor/normal brain tissue uptake ratio of MET correlated with the Mib-1 labeling index, which is a marker for proliferation. Thus, MET uptake in astrocytomas might be associated with tumor viability, and higher MET uptake might indicate a more aggressive type of astrocytoma tumor [24].

TABLE 2

Summary of key PET/SPECT imaging biomarker studies

PET/SPECT tracer	Approach	Purpose	Refs
^{18}Fluorine-2-deoxy-D-glucose (FDG)	Imaging of tumor and inflammation in xenograft rat model for glioma	Comparison between FDG, FLT and FET PET for discriminating between tumor and inflammation	[26]
L-(Methyl-^{11}C)methionine (MET)	Imaging of (suspected) primary or recurrent brain tumors in patients in combination with software reconstruction of biopsy trajectory	Determination if MET PET can detect infiltrating tumor parts	[23]
	Imaging of tumor in patients with grade II glioma before surgery	Determination of tumor viability and malignant transformation	[24]
O-(2-^{18}F-fluoroethyl)-L-tyrosine (FET)	Prospective evaluation of patients with head and neck squamous cell carcinoma	Comparison between FDG and FET PET imaging	[25]
^{18}F-labeled 1-amino-3-fluoro-cyclobutane carboxylic acid (FACBC)	Imaging of patients with (suspected) prostate carcinoma	Determination of FACBC uptake	[27]
^{11}C-Thymidine	Study of blood and tissue variability in patients that following ^{11}C-thymidine PET	Determination of ^{11}C-thymidine PET imaging reproducibility	[28]
^{18}F-3-fluoro-3-deoxy-thymidine (FLT)	Imaging of patients with non-small-cell lung cancer and head and neck cancer before treatment	Determination of FLT PET imaging reproducibility	[30]
^{11}C-choline	Imaging of patients with hepatocellular carcinoma	Comparison of FDG and ^{11}C-choline PET for detection of hepatocellular carcinoma	[31]
^{11}C-acetate (AC)	Imaging of patients with thyoma	Comparison of FDG and AC PET for predicting the histologic types and tumor invasiveness	[32]
^{18}F-fluoromisonidazole (FMISO)	Imaging of patients with glioblastoma multiforme before radiotherapy	Assessment of hypoxia impact on survival	[34]
Cu-diacetyl-bis(N4-methyl-thiosemicarbazone) (Cu-ATSM)	Imaging of patients with cervical cancer before radiotherapy	Confirmation that pretreatment tumor hypoxia is a biomarker for poor prognosis	[33]
^{18}F-fluoroestradiol (FES)	Imaging of patients with breast cancer and IHC on cancer tissue samples	Comparison of ER expression by FES PET and IHC	[36]
^{64}Cu-labeled DOTA-D-Phe^{1}-Tyr^{3}-octreotide (^{64}Cu-labeled DOTA-TOC)	Imaging of tumors in a xenograft mouse model for glioblastoma	Evaluation of imaging agent to assess somatostatin overexpressing tumors	[35]
^{124}I-HuMV833	Imaging of patients with various progressive solid tumors	Determination of distribution, pharmacokinetic properties and therapeutic effect of anti-VEGF antibody	[40]
^{68}Ga-1,4,7,10-tetraazacyclododecane-*N,N′,N″,N‴*-tetraacetic acid (DOTA)-Re(Arg^{11})CCMSH (^{68}Ga-DOTA-Re(Arg^{11})CCMSH)	Imaging of mice bearing syngeneic xenograft melanoma tumors	Detection of metastatic melanoma	[37]
^{124}I-affibody	Imaging of mice bearing gastric adenocarcinoma cell tumors derived from liver metastases overexpressing HER2	Comparison between ^{124}I-affibody and ^{125}I-trastuzumab PET for imaging of HER2 overexpressing tumors	[58]
^{18}F-galacto-RGD	Imaging of patients with different types of cancers	Comparison of integrin expression and glucose metabolism in patients with various types of cancers	[39]
^{64}Cu-DOTA-VEGF$_{121}$	Imaging of tumors in a xenograft mouse model for glioblastoma	Measure VEGFR-2 expression	[41]
^{124}I-minibody	Imaging of tumors in a xenograft mouse model for prostate cancer	Evaluation of imaging agent to detect PSCA-positive prostate tumors	[61]
^{124}I-diabody	Imaging of tumors in a xenograft mouse model for prostate cancer	Comparison of different diabodies for imaging of PSCA-positive prostate tumors	[62]

^{99m}Tc-anti-EGFR nanobody	SPECT imaging of xenograft mouse models of skin and prostate carcinoma	Imaging of tumors	[70,71]
^{99m}Tc-anti-EGFR affibody	SPECT imaging of in xenograft breast cancer mouse models	Imaging of HER2-positive tumors	[63]
^{111}In-DTPA trastuzumab	SPECT imaging in xenograft mouse models of breast cancer	Imaging of HER2-positive tumors and assessment of trastuzumab therapy	[56]
^{99m}Tc-anti-DR5 antibody	SPECT imaging in xenograft mouse models of breast cancer	Visualization of uptake and distribution of imaging agent in tumors	[54]
^{125}I-anti-CXCR4 antibody	SPECT/CT imaging in xenograft mouse models of glioblastoma	Imaging of CXCR4-positive tumors	[57]

Nevertheless, the inherent short half-life of ^{11}C has lead to the development of other radiolabeled amino acids, such as O-(2-^{18}F-fluoroethyl)-L-tyrosine (FET), and a non-metabolizable amino acid, ^{18}F-labeled 1-amino-3-fluoro-6-cyclobutane carboxylic acid (FACBC). Although a comparative study by Balagova *et al.* [25] in patients with head and neck squamous cell carcinoma revealed that FET PET is not suitable to replace FDG PET for diagnosis of head and neck cancer, it was demonstrated recently that FET PET was superior to FDG PET in differentiating tumor from inflammation [26]. Uptake of FACBC has also been demonstrated in primary and metastatic tumors of patients with prostate cancer [27].

As increased cellular proliferation is a characteristic of tumor cells, nucleoside metabolism can also be used as a target for PET tracers. In this context ^{11}C-thymidine was initially developed to assess tumor cell proliferation [28]. As previously mentioned, ^{11}C has a short half-life (20 min); therefore, to overcome this limitation, FLT was developed. FLT PET imaging has been demonstrated in patients with glioma. Uptake correlated with Mib-1 cellular proliferation labeling index, indicating the potential use of FLT as a marker for cellular proliferation in brain cancer. It was also shown, however, that FLT PET cannot accurately define tumor margins (also demonstrated with MET PET). This is probably the result of varied cell populations being present in gliomas. It seems that one population does not infiltrate but rapidly divides and, therefore, facilitates FLT uptake, whereas the other population does not proliferate but invades the surrounding tissue [29]. However, one recent study has demonstrated the reproducibility of quantitative FLT measurements. Patients with non-small-cell lung cancer or head and neck cancer underwent FLT PET imaging twice over a seven-day period. FLT PET reproducibly imaged all primary tumors and more than 90% of suspected locoregional metastases [30].

Lipid metabolism targeting PET tracers have also been developed, including ^{11}C-choline and ^{11}C-acetate. When ^{11}C-choline is taken up by the tumor, it is rapidly phosphorylated and trapped in the cell membrane. The feasibility of ^{11}C-choline PET was compared with FDG PET in patients with hepatocellular carcinoma. ^{11}C-choline PET showed improved detection rates in moderately differentiated tumors, whereas FDG PET showed better detection rates for poorly differentiated tumors [31]. Prediction of tumor invasiveness and histologic type of thyoma was assessed with FDG PET and ^{11}C-acetate. PET imaging was performed before surgery in patients with thyoma and measured as standard maximum uptake. Tumor invasiveness was assessed by pathologic tumor stage. Results demonstrated that although neither FDG PET nor ^{11}C-acetate PET could predict invasiveness of thyomas, both PET approaches were useful in determining the histologic type of thyoma present [32].

Tumor hypoxia

Tumor hypoxia is a key characteristic of human cancers and can be associated with more aggressive tumor types and poor prognosis. Furthermore, tumor hypoxia is associated with metastasis and chemotherapy resistance. Several tracers are currently under development for tumor hypoxia imaging. The most promising probes include Cu-diacetyl-bis(N^4-methylthiosemicarbazone) (Cu-ATSM) and ^{18}F-fluoromisonidazole (FMISO). Reduction of Cu-ATSM occurs in both hypoxic and normoxic cells. In normoxic cells

(in the presence of oxygen), however, Cu-ATSM is reoxidized and able to diffuse out of the cell. In hypoxic cells, Cu-ATSM is irreversibly trapped. Many preclinical and clinical studies have been performed using Cu-ATSM PET in a variety of cancer indications. Recently, Cu-ATSM PET imaging was used to show that pretreatment tumor hypoxia is a biomarker for poor prognosis in patients with cervical cancer. Patients with biopsy-proved cervical cancer underwent Cu-ATSM PET imaging, and resultant scan data indicated that tumor-to-muscle uptake ratios of Cu-ATSM were related to progression-free survival and cause-specific survival. Interestingly, no correlation was found between FDG uptake and Cu-ATSM uptake [33]. Several studies have demonstrated that FMISO is useful in detecting hypoxic tumors in various types of cancer. Spence *et al.* [34] have recently demonstrated the feasibility of FMISO PET imaging to measure hypoxia in patients with glioblastoma. Patients underwent FMISO PET before radiotherapy, and the volume and intensity of hypoxia and poorer time to progression and survival were correlated. One advantage of FMISO is that it can be reversibly reduced and reoxidized, enabling diffusion out of the cell. To date, however, several drawbacks of FMISO PET have limited its use in clinical settings; crucially, it has poor tissue uptake and slow cellular washout, delaying the imaging process.

Tumor receptor expression

Recently developed cancer therapeutics are based on specific targeting of molecular pathways and processes. This has lead to the development of several PET tracers that target expression/overexpression of receptors and proteins on tumor cells. Several important examples exist, including the development of radiolabeled somatostatin and estrogen receptor analogs [35,36]. Recently, PET imaging with ^{68}Ga-labeled peptide analogs that target MC1 receptors overexpressed on melanoma tumors has also been demonstrated. ^{68}Ga-labeled peptide analogs were administered to mice bearing B16 melanomas. Scan data clearly demonstrated rapid receptor-mediated tumor uptake, resulting in high-resolution tumor images. This application might be important in the future for early diagnosis of metastasized melanoma [37].

Inhibition of angiogenesis, the formation of new blood vessels from pre-existing vasculature, was first proposed as a therapeutic strategy against malignancies by Folkman in 1971 [38] and is now a well-established therapeutic strategy in oncology. As such, it is noteworthy that several PET probes have now also been developed in an attempt to functionally image this process. One approach is based on targeting of the αvβ3 integrin with the Arg-Gly-Asp (RGD) peptide. The αvβ3 integrin is upregulated at sites of neovascularization on endothelium and tumor cells and is an attractive target for tumor imaging and therapy. The potential of imaging expression of the αvβ3 integrin with ^{18}F-galacto-RGD was demonstrated and compared with FDG PET in patients with different primary and metastatic tumors. No correlation between FDG PET and ^{18}F-galacto-RGD PET was found, indicating that tumor glucose metabolism and αvβ3 integrin expression are not closely connected. FDG PET remains superior in tumor staging because it was more sensitive in tumor detection than ^{18}F-galacto-RGD PET. However, ^{18}F-galacto-RGD PET might be more useful in assessment of anti-angiogenic treatment [39].

Another approach towards imaging angiogenesis includes targeting of vascular endothelial growth factor (VEGF) receptor. VEGF binding to VEGF receptor 1 (VEGFR-1) and receptor 2 (VEGFR-2) are essential pathway in tumor angiogenesis and have been used for anti-cancer therapeutic targets. Recently, a humanized version of a mouse monoclonal VEGF antibody has been radiolabeled with ^{124}I to study the distribution, pharmacokinetics and therapeutic efficacy in patients. Data from PET imaging demonstrated a high degree of variation of antibody uptake and clearance for different tumors in the same patient. These variations could be responsible for the lack of efficacy in several tumor types and believed resistance against antibody-based anti-angiogenesis therapies. It was concluded that it is undesirable to compare patients with different or even the same tumor type after treatment with different doses of antibody [40].

Furthermore, the $VEGF_{121}$ isoform has been conjugated to 1,4,7,10-tetraazacyclododecane-1,4,7,10-tetraacetic acid (DOTA) and radiolabeled with ^{64}Cu. This PET tracer was used to image mice bearing glioblastoma xenograft tumors. Tumor uptake value of ^{64}Cu-DOTA-$VEGF_{121}$ correlated with relative tumor tissue expression of VEGFR-2. High uptake in kidneys was also seen, however – probably owing to high expression of VEGFR-1 in rodent kidneys. Further studies are required to translate use of this tracer into the clinic [41].

Note: No discussion on the feasibility of imaging angiogenesis *in vivo* would be complete without mentioning the process of

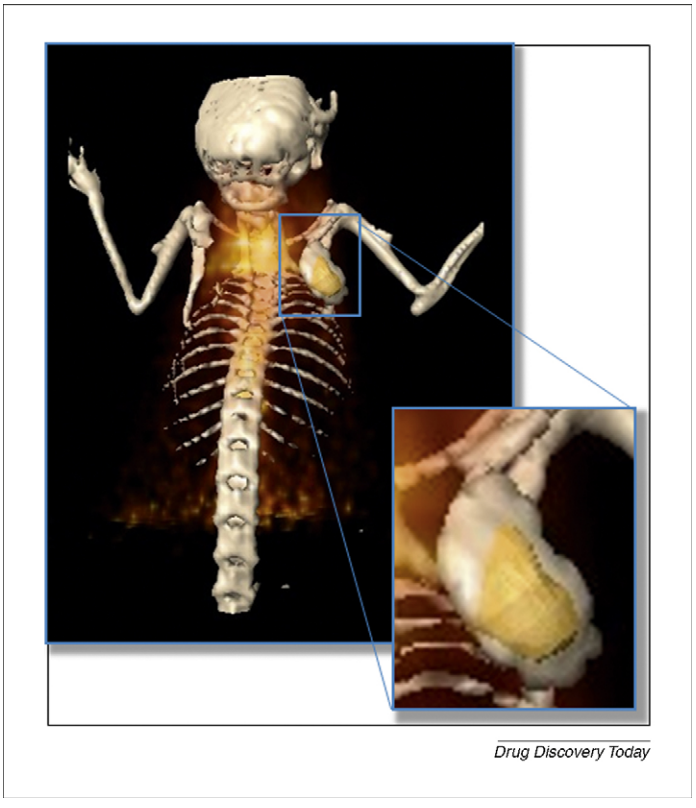

FIGURE 2

Multimodality imaging of Balb/C athymic nude mouse bearing human MCF-7 tumor xenograft. PET/CT overlay image was acquired on a FLEX Triumph multimodality preclinical platform (GE), 1 h after intravenous injection of 100 μCi ^{18}F-fluorodeoxyglucose (FDG). Shown is the coronal view of a tumor-bearing mouse demonstrating FDG uptake within a subcutaneous tumor above the right shoulder. Image courtesy of Tracee Terry, Kerrie H. Tainter and J. Michael Mathis, Gene and Cell Therapy Program, LSU Health Sciences Center in Shreveport, and the Biomedical Research Foundation of Northwest Louisiana.

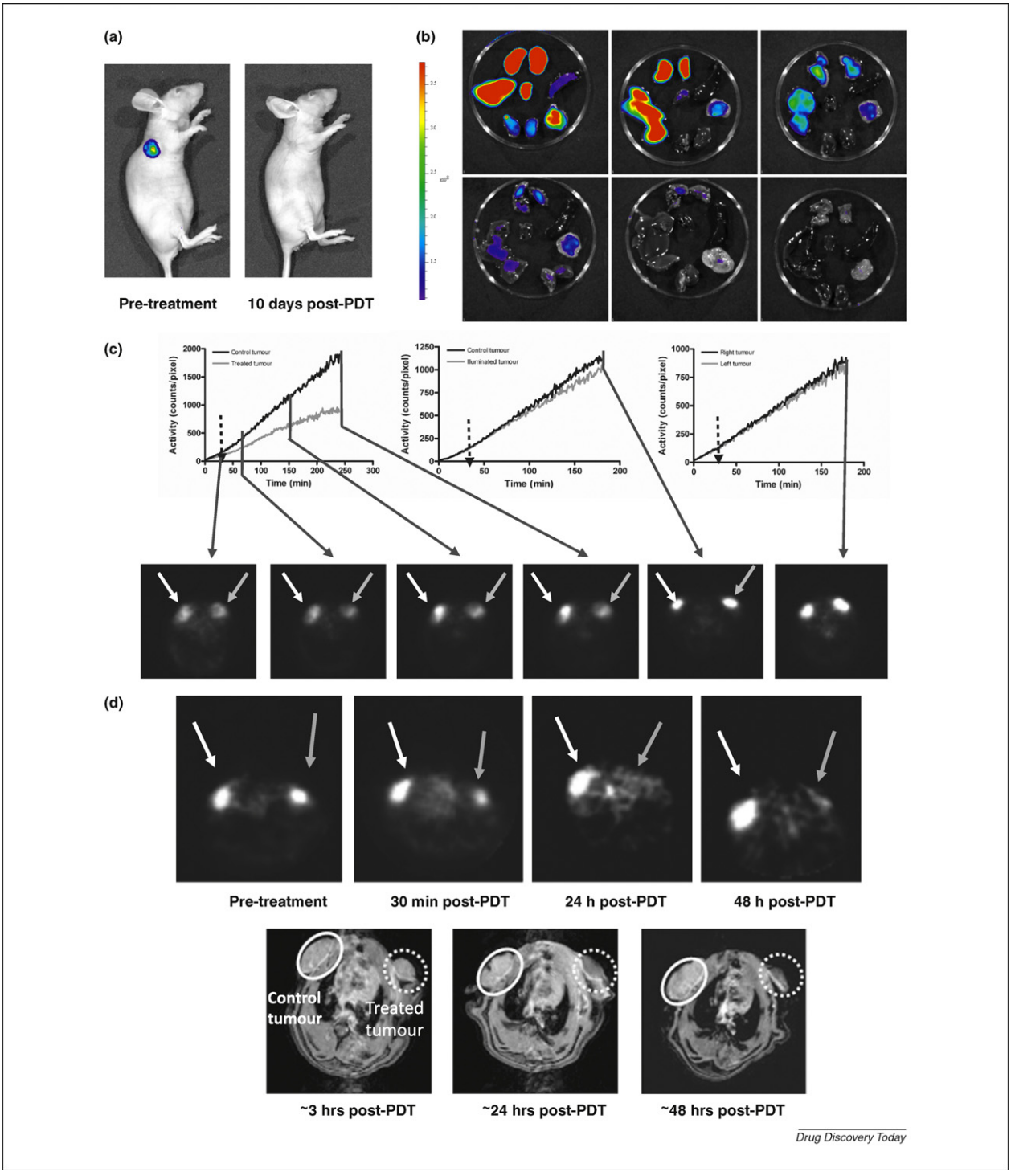

FIGURE 3

In vivo multimodality imaging of ADPM06 theranostic. *In vivo* and *ex vivo* optical imaging were performed using an IVIS Spectrum (Caliper LS) small animal imaging system. (a) Reduction in tumor fluorescence (photons/second/cm^2/steradian) of MDA-MB-231-GFP xenograft tumors 10 days after treatment with 2 mg/kg ADPM06 + 150 J/cm^2 light. (b) *In vivo* biodistribution of ADPM06, as measured by NIRF (690 nm). Mice bearing MDA-MB-231-luc tumors were euthanized over a 48 h interval after intravenous injection of 2 mg/kg ADPM06 and organs imaged *ex vivo*. Quantification of fluorescence intensity revealed a peak in ADPM06 fluorescence in all organs 15 min post-injection, with the exception of the liver, which reached maximum fluorescence at 1 h. Fluorescence intensity reached baseline levels by 24 h. Drug appeared to be cleared from the animal by 48 h. (c) Time–activity curves during ^{18}F-FDG infusion representing dynamic radiotracer uptake in rats bearing intradermal 13762 MAT B III-tumors in PDT (0.8 mg/kg ADPM06 + 150 J/cm^2), light alone (150 J/cm^2) and ADMP06 alone (0.8 mg/kg) treated animals. ^{18}F-FDG PET image slices through tumors taken at selected time points before and after treatment are also shown. PET imaging was performed on the FLEX Triumph preclinical PET platform (GE). Dynamic ^{18}F-FDG revealed that the mechanistic basis of the PDT treatment was consistent with a vascular targeted response through examination of transient changes in the ^{18}F-FDG uptake rate that occurred from 10 to 30 min after commencement of illumination. (d) Upper panel: changes in tumor hexokinase metabolism over a 48 h period after ADPM06-mediated PDT following bolus injection of 1.0–1.3 mCi ^{18}F-FDG. White arrows indicate the control tumor; grey arrows indicate treated tumors. Lower panel: MRI of control vs. PDT-treated animals show changes in tumor perfusion at ~3 h, 24 h and 48 h post-treatment Gd-DTPA MRI contrast agent was delivered parenterally before scanning. Image reprinted, with permission, from *British Journal of Cancer* [82].

DCE-MRI. MRI is based on the detection of nuclear spin realignment in an externally applied magnetic field. Signal enhancement is obtained with DCE-MRI, where a paramagnetic contrast agent is injected. The contrast agent influences the relaxation times of nearby hydrogen nuclei, resulting in signal enhancement. Monitoring tumor angiogenesis with DCE-MRI is based on the assessment of contrast agent pharmacokinetics as it passes through the tumor vasculature. With this technique, biomarkers of physiological processes and microvascular features such as flow, permeability and volume are provided. DCE-MRI itself is a potential biomarker for tumor angiogenesis. This technique is now incorporated in clinical trials to assess the therapeutic effect of angiogenesis inhibitors. However, differences in analysis methods and result interpretations might influence the predictive outcome of DCE-MRI. DCE-MRI and more recent techniques, such as MR spectroscopy and hyperpolarized carbon MR, have been recently discussed in detail [42].

Multimodality imaging

By combining MI modalities, additive information can be used to further assess disease progression when compared with the use of a single imaging modality alone. The combination of several imaging modalities, such as PET/CT and SPECT/CT, to assess disease progression is already widely used in the clinic [43]. By combining nuclear imaging with CT, anatomical information supplements high spatial resolution of nuclear tracer imaging (Figure 2).

At present, the major drawback with multimodality imaging systems such as PET/CT in clinical and preclinical settings is that imaging is performed sequentially and imaging data sets are combined by software. Most recently, research has focused on investigating the feasibility of combining two imaging modalities that image the same specimen at the same time. For example, Judenhofer *et al.* [44] have described the construction of a combined PET/MR imaging system for laboratory animals. This system uses a PET detector based on lutetium oxyorthosilicate scintillation crystals combined with compact solid-state silicon photosensors insensitive to magnetic fields. Simultaneous MRI and FLT PET imaging has been performed in a mouse model for colon carcinoma. FLT PET images showed highly proliferative areas of tumors, and the morphology of areas with lower PET tracer uptake – such as necrotic and inflammatory areas – could be visualized with MRI [44]. To date, several combination strategies are being used in translational studies. Combinations include MRI/optical imaging, nuclear imaging/optical imaging, and nuclear imaging/MRI [45]. However, clinical translation of these integrated systems might be difficult. The complexities associated with integrated system design for both preclinical and clinical scanners might be important. This is likely to result in high engineering costs and, thus, reduced feasibility for widespread laboratory and clinical installation, respectively. The combined toxicity of imaging agents for separate modalities could also prove to be an important issue. Therefore, an important advancement in the field is the development of multimodality imaging agents.

Lijowski *et al.* [46] have developed a dual-modality nanoparticle for imaging of tumor angiogenesis. Nanoparticles were assembled by preparing a lipid film of an αvβ3 integrin antagonist coupled to PEG, gadolinium diethylenetriamine-pentaacetic acid-bis-oleate, lecithin and phosphatidylethanolamine. The lipid film was rehydrated in water with emulsified perfluorooctylbromide nanoparticles to produce dual-modality imaging probes. Subsequently, the nanoparticle was labeled with ^{99m}Tc for SPECT imaging and gadolinium chelates were incorporated for MRI detection. Administration of these particles in Vx2 tumor-bearing rabbits showed that a discrete tumor neovasculature signal could be obtained. 3D mapping of angiogenesis could be performed using MRI, whereas CT imaging could not distinguish between tumor and lymph node. Another targeted nanoparticle approach has been used to image breast cancer. A fragment of urokinase-type plasminogen activator (uPa) was conjugated to magnetic iron oxide nanoparticles to target the uPa receptor, which is overexpressed in breast cancer tissues. Furthermore, the NIRF dye Cy5.5 was conjugated to the nanoparticle, enabling fluorescence imaging. Imaging characteristics of these particles were tested in syngeneic mouse models of breast tumors and metastases, and MRI results showed that the nanoparticles accumulated in primary and metastatic tumors. Tumor accumulation was confirmed with NIRF imaging [84].

The combination of PET and BLI has been demonstrated by Deroose *et al.* A tri-fusion reporter gene approach that allows detection of gene expression by fluorescence, BLI and PET imaging was employed. Human melanoma cell lines were lentivirally transfected with the tri-fusion reporter gene and inoculated in mice. Data indicated that metastatic tumors could be imaged at an early stage by BLI, and these tumors were later accurately localized on 3D PET/CT images, combining non-invasive gene reporter imaging with structural anatomical information [47].

The combination of BLI and MRI has been further shown in an orthotopic xenograft model for bladder cancer. Human bladder tumor cells lentivirally transfected to express the luciferase gene and subsequently inoculated in the bladder. Tumor burden of mice was imaged with BLI, which correlated with tumor volume measured by *ex vivo* MRI, and histological endpoint measurements [48].

Most recently, multimodality imaging approaches have been used in the development of optically active NIRF theranostics. The term 'theranostics' refers to the rapidly evolving notion of combining diagnostics with therapeutics. NIRF theranostics represent an emerging class of imaging biomarkers/therapeutics that might be activated *in vivo* to provide a personalized therapeutic response. A combination of BLI, PET and MRI has been used to study the therapeutic effect of the theranostic photosensitizer ADPM06, lead agent of the BF_2-chelated tetraaryl-azadipyrromethenes (ADPMs) class of theranostic photosensitizer [49–52] (Figure 3). First, mice were inoculated with human breast cancer cells, which expressed luciferase or GFP to examine drug distribution clearance and efficacy. FDG PET was subsequently used to assess mechanisms of therapeutic effect of ADPM06 in rats bearing mammary tumors, where an almost complete suppression of metabolic tumor activity was observed at 24 h and 48 h post photodynamic treatment. MRI was further used to study the effects of ADPM06 treatment on tumor vascular perfusion. Results showed a clear difference in accumulation of MRI contrast agent between control and treated rats, indicating that ADPM06-treated tumors have an overall vascular-targeting effect [82].

New development focus: antibody fragments as disease progression imaging biomarkers

Monoclonal antibodies (mAbs) have been employed as targeted therapeutic molecules for several years. Their therapeutic effect is

mediated by blocking of a signaling pathway that represents a determinant of disease progression and/or by inducing antibody-dependent cell-mediated cytotoxicity. MAbs have also long been employed for tumor imaging [53–60]. Their remarkable specificity in target binding and identification of antigens particularly over-expressed on tumor cells has enabled discrimination between tumors and normal tissues.

For imaging applications, probe size (hydrodynamic diameter and molecular weight) is a determinant factor for biodistribution and clearance. Other factors also influence tumor detection by antibodies or fragments, including antigen affinity, binding accessibility and the fate of the probe upon cell binding. Engineering technologies have thus been employed to modify the size, pharmacokinetics, avidity, affinity and immunogenicity of mAbs. As a result, a variety of antibody fragments have been generated, for which imaging is one of the key applications. These fragments include single-chain variable fragments (scFv, 25 kDa, *t* 1/2 life 0.5–2.0 h), diabodies (55 kDa, *t* 1/2 life 3–7 h) and minibodies (80 kDa, *t* 1/2 life 6–11 h).

Leyton et al. have employed a minibody approach to image prostate cancer in a preclinical xenograft model. The ^{124}I-labeled minibody recognizing prostate stem cell antigen (PSCA) enabled imaging of the tumors with PET 21 h after injection. This time interval was much shorter than that generally required when intact anti-PSCA antibody is employed (up to seven days) [61]. Most recently, the same group has developed and tested a variety of diabodies recognizing the same target [62]. The best images and highest tumor-to-background ratios were obtained, by PET, 12 h after the injection of the ^{124}I-labeled diabodies. Both studies emphasize the advantage of developing small antibody fragments for early tumor molecular imaging, although it should also be noted that the smaller the antibody fragment employed, the lower the overall tumor accumulation. Nevertheless, antibody fragments smaller than diabodies have been successfully employed for tumor imaging. Affibodies are high-affinity 6 kDa molecules with simple and robust structure. Initially derived from one of the IgG-binding domains of staphylococcal protein A, affibodies have been developed for both therapeutic and imaging applications. In a recent study, ^{124}I-labeled trastuzumab was compared to a ^{124}I-labeled anti-HER2 affibody for imaging of HER2-expressing xenografts in nude mice [58]. The authors showed that tumor uptake was higher for trastuzumab, although higher tumor-to-background ratios were obtained with the affibody because of its rapid blood clearance. In fact, images obtained 72 h after injection of trastuzumab presented less contrast than images taken 6 h after the injection of the affibody. Other studies have investigated affibodies for cancer imaging, mainly targeting HER2 and EGFR, employing radioactive technologies but also near-infrared optical imaging [63–67]. A recent study has shown the production of multivalent affibodies by combining the specificity of two smaller fragments targeting HER2 and EGFR simultaneously. This could increase the chance of detecting tumor cells by finding one of the possible overexpressed growth factor receptors in comparison to a monovalent affibody approach [68].

Nanobodies are small antibody fragments (15 kDa) derived from the naturally occurring heavy-chain-only antibodies, first identified in llamas [69]. These fragments have also been referred to as VHH, as they consist of the variable domain (V_H) of the heavy-chain (H) antibodies. Even though their molecular weight is tenfold lower than that of mAbs, nanobodies are able to bind as specifically and as firmly as mAbs, with dissociation constants in the picomolar range. Furthermore, nanobodies are more resistant to temperature variations and acidic environments and are more soluble than scFv. Early studies indicate the potential of nanobodies for imaging applications; Huang and co-workers have demonstrated selective *in vivo* SPECT imaging of EGFR using a ^{99m}Tc-labeled anti-EGFR nanobody. This nanobody permitted imaging at early time points owing to its rapid blood clearance (half-life of 1.5 h) and accumulated three times more in the EGFR-overexpressing tumor model A431, as compared with the DU145 xenografts [70]. A separate study compared the biodistribution and tumor targeting of two ^{99m}Tc-labeled anti-EGFR nanobodies using pinhole SPECT and micro-CT. The rapid clearance of the unbound nanobodies enabled tumor-to-background ratios of ~32 as early as 1 h after the injection. *Ex vivo* biodistribution analysis 1.5 h after the injection revealed that ~9%IA/g were present in the tumor and that liver uptake was low (~1.5%IA/g) [71].

Tissue-based imaging in oncology biomarker discovery and validation

Over the past several years, there has been a noteworthy resurgence of interest in *ex vivo*/tissue-based imaging in the oncology biomarker arena. Mass spectrometry-based imaging [72] and infrared spectroscopy [73,74] of tissues have emerged as two highly innovative approaches that provide key information regarding the biodistribution of molecules of interest (e.g. proteins, lipids) without the requirement for prior labeling. Although both approaches have been used successfully to subclassify human tumor tissues and predict patient outcome in a research setting, there are considerable issues relating to validation of these technologies that must be resolved before they can be successfully translated into routine clinical analysis.

However, automated image analysis approaches to advance histopathological recognition and quantitation of biomarkers have gained considerable traction in recent years [75]; several approaches are on the cusp of widespread clinical implementation. With the advent of digital slide scanning technologies, the practice of pathology has started to undergo a paradigm shift, with classical logistical barriers to rapid sharing of data starting to be removed. Another driver in this agenda within the oncological area is the increasing use of tissue microarray technology, which enables the simultaneous analysis of hundreds of clinical specimens on a single microscope slide [76]. This has presented a key bottleneck in the manual interpretation of immunohistochemical (IHC) data, which automated image analysis approaches aim to resolve; similar issues are also being faced with fluorescence *in situ* hybridization (FISH) data. Indeed, such automated approaches are also starting to deliver valuable information in relation to quantitation of cancer biomarkers at a subcellular compartmental level [77–81] (Figure 4). For example, Brennan *et al.* [79] were able to quantify the expression of both nuclear and cytoplasmic Survivin (a central member of the inhibitor of apoptosis family of proteins) in a cohort of breast tumor specimens, showing that the nuclear form of this protein is associated with poor prognosis. More recently, Rexhepaj *et al.* [81] developed a unique approach for unsupervised (i.e. requiring minimal training) quantification of

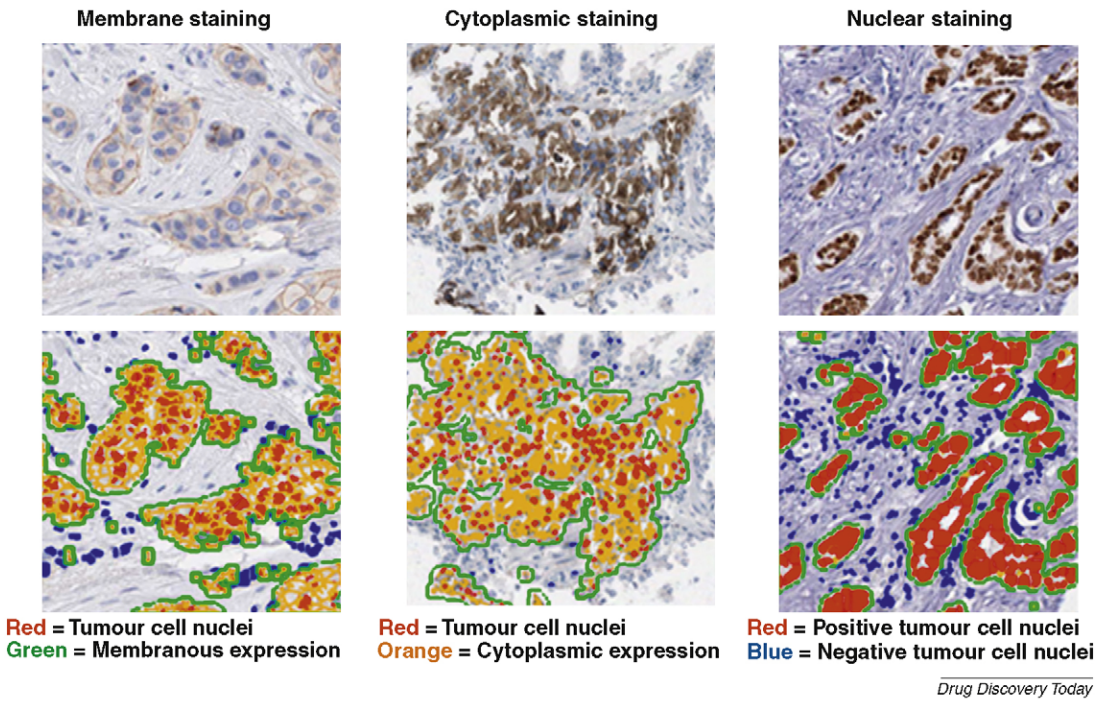

FIGURE 4

Application of automated image analysis approaches for quantification of cancer biomarkers at the subcellular compartment level. The upper panels show snapshots of cancer tissue specimens that have been immunohistochemically stained for either membrane, cytoplasmic or nuclear biomarkers. The lower panels show equivalent sections with marked up images, illustrating the application of automated image analysis approaches. Image courtesy of Elton Rexhepaj, University College Dublin.

estrogen and progesterone receptor (ER and PR, respectively) in >700 breast cancers. This study revealed good correlation between both manual and automated scoring data for both steroid receptors. Moreover, using specimens from a randomized control tamoxifen trial, these investigators also illustrated that automatically quantified ER retained its value as a predictive marker of drug response.

Key areas under development include approaches to distinguish tumor cells from non-tumor cells (e.g. stroma, inflammatory cells) within target tissue, as well as the creation of user-friendly interfaces to widen access to the technology. With respect to clinical implementation, several companies (Genetix, Aperio and BioImagene) have received FDA clearance for the use of HER2 FISH and IHC quantification algorithms [75]. Aperio also recently received approval from the FDA for the use of IHC quantification algorithms for ER and PR. The development of automated image analysis approaches for IHC quantification of cancer biomarkers is also being accelerated by the increasing focus on IHC surrogates in place of omic-based assays [78]. Although the gold standard in the immediate future is likely to remain the pathologist's eye, automated image analysis approaches are starting to be more widely accepted in the clinical community as decision support systems that can both fast-track and streamline this key step in biomarker evaluation.

Concluding remarks and future directions

An enhanced understanding of the molecular genesis of cancer, as well as the increasing superiority of imaging technologies, crucially assist translational researchers and clinicians in disease progression monitoring, thus enabling patients to engage in preventative and/or disease-retarding treatment regimens. The process of biomarker clinical translation is both complex and time-consuming. Multiple and diverse technologies play an integrated part in the process; the 'omics' platforms (genomics, proteomics, metabolomics and glyo-omics), *in vivo* molecular imaging strategies and evolving techniques such as tissue-based imaging have facilitated important clinical and preclinical advances in the field. This review has discussed the important role assigned to imaging in the cancer progression biomarker arena, highlighting some of the most crucial findings recently elucidated. Some of these techniques are already being used extensively in clinical settings such as FDG PET, although others, such as optical imaging and certain novel radiotracers, still face challenges in clinical translation.

Following recent advances with respect to NIRF *in vivo* imaging technologies (e.g. application of FMT), it is now likely that this emerging field will take increasingly progressive steps towards the clinic over the next several years. The application of theranostics (of which NIRF optically active agents represent an emerging subcategory) transcends the capabilities of straightforward imaging biomarkers or targeted therapeutics and promises a future of predictive personalized medicine in oncology and other life-threatening indications.

Although nuclear imaging has been used for several decades to detect and monitor tumors clinically, recently improved guidelines in the USA by the FDA for radiopharmaceutical development should now expedite the clinical translation of novel emerging disease progression tracers, some of which have been discussed in

the context of the current article. Moreover, the continued development of novel imaging approaches such as the use of small antibody fragments possessing favorable accumulation and imaging characteristics provide additional promise. The hybrid combination of complementary imaging modalities and future development of multimodality imaging probes will continue to push boundaries in the field.

Finally, tissue-based imaging has recently gained considerable traction within the medical diagnostics community, with several image analysis techniques now approved for clinical use. A key area of future development is centered on the use of fluorescence-oriented assays to better facilitate quantitation and simultaneous assessment of multiple markers. As previously mentioned, other tissue-imaging strategies (such as mass spectrometry or infrared spectroscopy) are on the horizon. These approaches might remove the requirement for antibody-based assessment of molecular characteristics within tissue specimens.

Conflict of interest statement

W.G. and A.B. hold shares in OncoMark Limited, a private company focused on cancer diagnostics. In addition, W.G. holds pending intellectual property in relation to the development of novel automated image analysis approaches in histopathology.

Acknowledgements

Funding is acknowledged from Science Foundation Ireland in the context of the Molecular Therapeutics for Cancer Ireland, Strategic Research Cluster and a Research Frontiers Programme Award. Funding is also acknowledged from the Irish Health Research Board in the context of a Programme Grant award: Breast Cancer Metastasis: Biomarkers and Functional Mediators. We further acknowledge funding received from the EU: Marie Curie Transfer of Knowledge Industry–Academia Partnership and Pathways programme – Target-Breast (http://www.targetbreast.com).

References

1 (2001) Biomarkers Definitions Working Group. Biomarkers and surrogate endpoints: preferred definitions and conceptual framework. *Clin. Pharmacol. Ther.* 69, 89–95
2 World Health Organization (1979) *WHO handbook for reporting results of cancer treatment*. WHO offset publication 48, WHO
3 Therasse, P. *et al.* (2000) New guidelines to evaluate the response to treatment in solid tumors. European Organization for Research and Treatment of Cancer, National Cancer Institute of the United States, National Cancer Institute of Canada. *J. Natl. Cancer Inst.* 92, 205–216
4 Eisenhauer, E.A. *et al.* (2009) New response evaluation criteria in solid tumours: revised RECIST guideline (version 1.1). *Eur. J. Cancer* 45, 228–247
5 Karrison, T.G. *et al.* (2007) Design of phase II cancer trials using a continuous endpoint of change in tumor size: application to a study of sorafenib and erlotinib in non small-cell lung cancer. *J. Natl. Cancer Inst.* 99, 1455–1461
6 Choi, H. *et al.* (2007) Correlation of computed tomography and positron emission tomography in patients with metastatic gastrointestinal stromal tumor treated at a single institution with imatinib mesylate: proposal of new computed tomography response criteria. *J. Clin. Oncol.* 25, 1753–1759
7 Zinn, K.R. *et al.* (2008) Noninvasive bioluminescence imaging in small animals. *ILAR J.* 49, 103–115
8 Zhao, D. *et al.* (2008) Antivascular effects of combretastatin A4 phosphate in breast cancer xenograft assessed using dynamic bioluminescence imaging and confirmed by MRI. *FASEB J.* 22, 2445–2451
9 Hsieh, C.L. *et al.* (2007) Non-invasive bioluminescent detection of prostate cancer growth and metastasis in a bigenic transgenic mouse model. *Prostate* 67, 685–691
10 Liao, C.P. *et al.* (2007) Mouse models of prostate adenocarcinoma with the capacity to monitor spontaneous carcinogenesis by bioluminescence or fluorescence. *Cancer Res.* 67, 7525–7533
11 Rao, J. *et al.* (2007) Fluorescence imaging *in vivo*: recent advances. *Curr. Opin. Biotechnol.* 18, 17–25
12 Diagaradjane, P. *et al.* (2008) Imaging epidermal growth factor receptor expression *in vivo*: pharmacokinetic and biodistribution characterization of a bioconjugated quantum dot nanoprobe. *Clin. Cancer Res.* 14, 731–741
13 Makino, A. *et al.* (2009) Near-infrared fluorescence tumor imaging using nanocarrier composed of poly(L-lactic acid)-block-poly(sarcosine) amphiphilic polydepsipeptide. *Biomaterials* 30 (28), 5156–5160
14 Papagiannaros, A. *et al.* (2009) Near infrared planar tumor imaging and quantification using nanosized Alexa 750-labeled phospholipid micelles. *Int. J. Nanomedicine* 4, 123–131
15 Lo, P.C. *et al.* (2009) Photodynamic molecular beacon triggered by fibroblast activation protein on cancer-associated fibroblasts for diagnosis and treatment of epithelial cancers. *J. Med. Chem.* 52, 358–368
16 Korideck, H. and Peterson, J.D. (2009) Noninvasive quantitative tomography of the therapeutic response to dexamethasone in ovalbumin-induced murine asthma. *J. Pharmacol. Exp. Ther.* 329, 882–889
17 Krautz-Peterson, G. *et al.* (2009) Imaging schistosomes *in vivo*. *FASEB J.* 23, 2673–2680
18 McCann, C.M. *et al.* (2009) Combined magnetic resonance and fluorescence imaging of the living mouse brain reveals glioma response to chemotherapy. *Neuroimage* 45, 360–369
19 Montet, X. *et al.* (2005) Tomographic fluorescence mapping of tumor targets. *Cancer Res.* 65, 6330–6336
20 Chowdhury, F.U. and Scarsbrook, A.F. (2008) The role of hybrid SPECT-CT in oncology: current and emerging clinical applications. *Clin. Radiol.* 63, 241–251
21 Mawlawi, O. and Townsend, D.W. (2009) Multimodality imaging: an update on PET/CT technology. *Eur. J. Nucl. Med. Mol. Imaging* 36 (Suppl. 1), S15–S29
22 Spanoudaki, V.C. and Ziegler, S.I. (2008) PET & SPECT instrumentation. *Handb. Exp. Pharmacol.* 185, 53–74
23 Kracht, L.W. *et al.* (2004) Delineation of brain tumor extent with [11C]L-methionine positron emission tomography: local comparison with stereotactic histopathology. *Clin. Cancer Res.* 10, 7163–7170
24 Kato, T. *et al.* (2008) Analysis of 11C-methionine uptake in low-grade gliomas and correlation with proliferative activity. *AJNR Am. J. Neuroradiol.* 29, 1867–1871
25 Balogova, S. *et al.* (2008) Prospective comparison of FDG and FET PET/CT in patients with head and neck squamous cell carcinoma. *Mol. Imaging Biol.* 10, 364–373
26 Lee, T.S. *et al.* (2009) Comparison of 18F-FDG, 18F-FET and 18F-FLT for differentiation between tumor and inflammation in rats. *Nucl. Med. Biol.* 36, 681–686
27 Schuster, D.M. *et al.* (2007) Initial experience with the radiotracer anti-1-amino-3-18F-fluorocyclobutane-1-carboxylic acid with PET/CT in prostate carcinoma. *J. Nucl. Med.* 48, 56–63
28 Wells, P. *et al.* (2005) 2-[11C]thymidine positron emission tomography reproducibility in humans. *Clin. Cancer Res.* 11, 4341–4347
29 Price, S.J. *et al.* (2009) Imaging regional variation of cellular proliferation in gliomas using 3′-deoxy-3′-[18F]fluorothymidine positron-emission tomography: an image-guided biopsy study. *Clin. Radiol.* 64, 52–63
30 de Langen, A.J. *et al.* (2009) Reproducibility of quantitative 18F-3′-deoxy-3′-fluorothymidine measurements using positron emission tomography. *Eur. J. Nucl. Med. Mol. Imaging* 36, 389–395
31 Yamamoto, Y. *et al.* (2008) Detection of hepatocellular carcinoma using 11C-choline PET: comparison with 18F-FDG PET. *J. Nucl. Med.* 49, 1245–1248
32 Shibata, H. *et al.* (2009) 18F-fluorodeoxyglucose and 11C-acetate positron emission tomography are useful modalities for diagnosing the histologic type of thymoma. *Cancer* 115, 2531–2538
33 Dehdashti, F. *et al.* (2008) Assessing tumor hypoxia in cervical cancer by PET with 60Cu-labeled diacetyl-bis(N4-methylthiosemicarbazone). *J. Nucl. Med.* 49, 201–205
34 Spence, A.M. *et al.* (2008) Regional hypoxia in glioblastoma multiforme quantified with [18F]fluoromisonidazole positron emission tomography before radiotherapy: correlation with time to progression and survival. *Clin. Cancer Res.* 14, 2623–2630
35 Hanaoka, H. *et al.* (2009) Evaluation of (64)Cu-labeled DOTA-D-Phe(1)-Tyr (3)-octreotide ((64)Cu-DOTA-TOC) for imaging somatostatin receptor-expressing tumors. *Ann. Nucl. Med.* 23 (6), 559–567

36 Peterson, L.M. *et al.* (2008) Quantitative imaging of estrogen receptor expression in breast cancer with PET and 18F-fluoroestradiol. *J. Nucl. Med.* 49, 367–374
37 Cantorias, M.V. *et al.* (2009) Development of high-specific-activity (68)Ga-labeled DOTA-rhenium-cyclized alpha-MSH peptide analog to target MC1 receptors overexpressed by melanoma tumors. *Nucl. Med. Biol.* 36, 505–513
38 Folkman, J. (1971) Tumor angiogenesis: therapeutic implications. *N. Engl. J. Med.* 285, 1182–1186
39 Beer, A.J. *et al.* (2008) Comparison of integrin alphaVbeta3 expression and glucose metabolism in primary and metastatic lesions in cancer patients: a PET study using 18F-galacto-RGD and 18F-FDG. *J. Nucl. Med.* 49, 22–29
40 Jayson, G.C. *et al.* (2002) Molecular imaging and biological evaluation of HuMV833 anti-VEGF antibody: implications for trial design of antiangiogenic antibodies. *J. Natl. Cancer Inst.* 94, 1484–1493
41 Chen, K. *et al.* (2009) Quantitative PET imaging of VEGF receptor expression. *Mol. Imaging Biol.* 11, 15–22
42 Brindle, K. (2008) New approaches for imaging tumour responses to treatment. *Nat. Rev. Cancer* 8, 94–107
43 Bockisch, A. *et al.* (2009) Hybrid imaging by SPECT/CT and PET/CT: proven outcomes in cancer imaging. *Semin. Nucl. Med.* 39, 276–289
44 Judenhofer, M.S. *et al.* (2008) a new approach for functional and morphological imaging. *Nat. Med.* 14, 459–465
45 Cherry, S.R. (2009) Multimodality imaging: beyond PET/CT and SPECT/CT. *Semin. Nucl. Med.* 39, 348–353
46 Lijowski, M. *et al.* (2009) High sensitivity: high-resolution SPECT-CT/MR molecular imaging of angiogenesis in the Vx2 model. *Invest. Radiol.* 44, 15–22
47 Deroose, C.M. *et al.* (2007) Multimodality imaging of tumor xenografts and metastases in mice with combined small-animal PET, small-animal CT, and bioluminescence imaging. *J. Nucl. Med.* 48, 295–303
48 Hadaschik, B.A. *et al.* (2007) A validated mouse model for orthotopic bladder cancer using transurethral tumour inoculation and bioluminescence imaging. *BJU Int.* 100, 1377–1384
49 Gallagher, W.M. *et al.* (2005) A potent nonporphyrin class of photodynamic therapeutic agent: cellular localisation, cytotoxic potential and influence of hypoxia. *Br. J. Cancer* 92, 1702–1710
50 Gorman, A. *et al.* (2004) In vitro demonstration of the heavy-atom effect for photodynamic therapy. *J. Am. Chem. Soc.* 126, 10619–10631
51 Killoran, J. *et al.* (2002) Synthesis of BF2 chelates of tetraarylazadipyrromethenes and evidence for their photodynamic therapeutic behaviour. *Chem. Commun. (Camb.)* 17, 1862–1863
52 McDonnell, S.O. *et al.* (2005) Supramolecular photonic therapeutic agents. *J. Am. Chem. Soc.* 127, 16360–16361
53 Chen, T.J. *et al.* (2009) Targeted Herceptin-dextran iron oxide nanoparticles for noninvasive imaging of HER2/neu receptors using MRI. *J. Biol. Inorg. Chem.* 14, 253–260
54 Kim, H. *et al.* (2007) High-resolution single-photon emission computed tomography and X-ray computed tomography imaging of Tc-99m-labeled anti-DR5 antibody in breast tumor xenografts. *Mol. Cancer Ther.* 6, 866–875
55 Liu, S. *et al.* (2009) A novel type of dual-modality molecular probe for MR and nuclear imaging of tumor: preparation, characterization and *in vivo* application. *Mol. Pharm.* 6, 1074–1082
56 McLarty, K. *et al.* (2009) Associations between the uptake of 111In-DTPA-trastuzumab HER2 density and response to trastuzumab (Herceptin) in athymic mice bearing subcutaneous human tumour xenografts. *Eur. J. Nucl. Med. Mol. Imaging* 36, 81–93
57 Nimmagadda, S. *et al.* (2009) Immunoimaging of CXCR4 expression in brain tumor xenografts using SPECT/CT. *J. Nucl. Med.* 50, 1124–1130
58 Orlova, A. *et al.* (2009) On the selection of a tracer for PET imaging of HER2-expressing tumors: direct comparison of a 124I-labeled affibody molecule and trastuzumab in a murine xenograft model. *J. Nucl. Med.* 50, 417–425
59 Sampath, L. *et al.* (2007) Dual-labeled trastuzumab-based imaging agent for the detection of human epidermal growth factor receptor 2 overexpression in breast cancer. *J. Nucl. Med.* 48, 1501–1510
60 Sodee, D.B. *et al.* (2007) Synergistic value of single-photon emission computed tomography/computed tomography fusion to radioimmunoscintigraphic imaging of prostate cancer. *Semin. Nucl. Med.* 37, 17–28
61 Leyton, J.V. *et al.* (2008) Humanized radioiodinated minibody for imaging of prostate stem cell antigen-expressing tumors. *Clin. Cancer Res.* 14, 7488–7496
62 Leyton, J.V. *et al.* (2009) Engineered humanized diabodies for microPET imaging of prostate stem cell antigen-expressing tumors. *Protein Eng. Des. Sel.* 22, 209–216
63 Ahlgren, S. *et al.* (2009) Targeting of HER2-expressing tumors with a site-specifically 99mTc-labeled recombinant affibody molecule ZHER2:2395, with C-terminally engineered cysteine. *J. Nucl. Med.* 50, 781–789
64 Kramer-Marek, G. *et al.* (2009) Changes in HER2 expression in breast cancer xenografts after therapy can be quantified using PET and 18F-labeled affibody molecules. *J. Nucl. Med.* 50, 1131–1139
65 Kramer-Marek, G. *et al.* (2008) [18F]FBEM-Z(HER2:342)-Affibody molecule—a new molecular tracer for *in vivo* monitoring of HER2 expression by positron emission tomography. *Eur. J. Nucl. Med. Mol. Imaging* 35, 1008–1018
66 Lee, S.B. *et al.* (2008) Affibody molecules for *in vivo* characterization of HER2-positive tumors by near-infrared imaging. *Clin. Cancer Res.* 14, 3840–3849
67 Tolmachev, V. *et al.* (2009) Affibody molecules for epidermal growth factor receptor targeting *in vivo*: aspects of dimerization and labeling chemistry. *J. Nucl. Med.* 50, 274–283
68 Friedman, M. *et al.* (2009) Engineering and characterization of a bispecific HER2xEGFR-binding affibody molecule. *Biotechnol. Appl. Biochem.* 54, 121–131
69 Hamers-Casterman, C. *et al.* (1993) Naturally occurring antibodies devoid of light chains. *Nature* 363, 446–448
70 Huang, L. *et al.* (2008) SPECT imaging with 99mTc-labeled EGFR-specific nanobody for *in vivo* monitoring of EGFR expression. *Mol. Imaging Biol.* 10, 167–175
71 Gainkam, L.O. *et al.* (2008) Comparison of the biodistribution and tumor targeting of two 99mTc-labeled anti-EGFR nanobodies in mice, using pinhole SPECT/micro-CT. *J. Nucl. Med.* 49, 788–795
72 Cornett, D.S. *et al.* (2007) MALDI imaging mass spectrometry: molecular snapshots of biochemical systems. *Nat. Methods* 4, 828–833
73 Fernandez, D.C. *et al.* (2005) Infrared spectroscopic imaging for histopathologic recognition. *Nat. Biotechnol.* 23, 469–474
74 Petter, C.H. *et al.* (2009) Development and application of Fourier-transform infrared chemical imaging of tumour in human tissue. *Curr. Med. Chem.* 16, 318–326
75 Mulrane, L. *et al.* (2008) Automated image analysis in histopathology: a valuable tool in medical diagnostics. *Expert Rev. Mol. Diagn.* 8, 707–725
76 Brennan, D.J. *et al.* (2007) Contribution of DNA and tissue microarray technology to the identification and validation of biomarkers and personalised medicine in breast cancer. *Cancer Genomics Proteomics* 4, 121–134
77 Brennan, D.J. *et al.* (2009) The transcription factor Sox11 is a prognostic factor for improved recurrence-free survival in epithelial ovarian cancer. *Eur. J. Cancer* 45, 1510–1517
78 Brennan, D.J. and Gallagher, W.M. (2008) Prognostic ability of a panel of immunohistochemistry markers – retailoring of an 'old solution'. *Breast Cancer Res.* 10, 102
79 Brennan, D.J. *et al.* (2008) Altered cytoplasmic-to-nuclear ratio of survivin is a prognostic indicator in breast cancer. *Clin. Cancer Res.* 14, 2681–2689
80 Lanigan, F. *et al.* (2009) Increased claudin-4 expression is associated with poor prognosis and high tumour grade in breast cancer. *Int. J. Cancer* 124, 2088–2097
81 Rexhepaj, E. *et al.* (2008) Novel image analysis approach for quantifying expression of nuclear proteins assessed by immunohistochemistry: application to measurement of oestrogen and progesterone receptor levels in breast cancer. *Breast Cancer Res.* 10, R89
82 Byrne, A.T. *et al.* (2009) Vascular-targeted photodynamic therapy with BF2-chelated Tetraaryl-Azadipyrromethene agents: a multi-modality molecular imaging approach to therapeutic assessment. *Br. J. Cancer* 101 (9), 1565–1573
83 O'Neill, K. *et al.* (2009) Bioluminescent imaging: a critical tool in pre-clinical oncology research. *J. Pathol.*
84 Yang, L. *et al.* (2009) Receptor-targeted nanoparticles for in vivo imaging of breast cancer. *Clin. Cancer Res.* 15 (14), 4722–4732